ELSEVIER

Computers and Geotechnics 30 (2003) 419–430

COMPUTERS AND GEOTECHNICS

www.elsevier.com/locate/compgeo

Stability of an undrained plane strain heading revisited

Charles E. Augarde[a,*], Andrei V. Lyamin[b], Scott W. Sloan[b]

[a] *School of Engineering, University of Durham, UK*

[b] *Department of Civil, Surveying and Environmental Engineering, University of Newcastle, NSW 2308, Australia*

Received 19 July 2002; received in revised form 25 October 2002; accepted 9 January 2003

Abstract

The stability of an idealised heading in undrained soil conditions is investigated in this paper. The heading is rigidly supported along its length, while the face, which may be pressurised, is free to move. The problem approximates any flat wall in an underground excavation. Failure of the heading is initiated by a surface surcharge, acting with the self-weight of the soil. Finite element limit analysis methods, based on classical plasticity theory, are used to derive rigorous bounds on load parameters, for a wide range of heading configurations and ground conditions. Solutions for undrained soils with constant strength, and increasing strength with depth are presented. Recent improvements to finite element limit analysis methods, developed at the University of Newcastle, have allowed close bounds to be drawn in most cases. Previous research in this area has often been presented in terms of a stability ratio, N that combines load and self-weight into a single parameter. The use of a stability ratio for this problem is shown not to be rigorous, a finding that may be applicable to other stability problems in underground geomechanics.

Keywords: Stability; Heading; Limit analysis; Tunnel; Plasticity

1. Introduction

The assessment of the safety of shallow underground excavations in soft ground, for tunnel construction and mining, usually requires solutions to two separate predictive problems. Firstly, it is necessary to determine the stability of the excavation, for the safety of those at the surface and underground. Secondly, to prevent damage to surface or subsurface structures, it is also necessary to determine the pattern of ground deformations that will result from the construction works.

This paper presents the results of an investigation into the first of these problems as it affects what we will term a ''plane strain heading'' as shown in Fig. 1. This relatively simple configuration is applicable to a long-wall mining operation or to any flat wall in an underground excavation. While the problem of underground excavation stability is inherently three-dimensional, much can be learned from the behaviour of simpler two-dimensional models such as the one used in this paper. It consists of a plane strain idealisation of a long vertical open face, behind which the ground is supported by a rigid, and infinitely strong, lining. In practice, mines are supported by jacks or props spaced at close intervals to prevent cave-in. While these systems are not totally rigid, it seems reasonable to assume so here as this study is concerned with stability of the open face, rather than the determination of deformations. (Similar impractical assumptions are accepted for many problems in geomechanics, for instance ''rigid'' footings). An alternative plane strain model of an underground excavation is obtained by an orthogonal view to that shown in Fig. 1, although in that case the excavation must be unlined. Neither plane strain models capture the three-dimensional nature of an underground excavation but are still useful tools given the difficulties in using fully three-dimensional models.

In the work presented here, numerical procedures are used to find bounds on parameters describing the stability of a range of heading sizes in undrained soil conditions. The procedures used here are based on the limit theorems of classical plasticity, using discretisations similar to the displacement finite element method. Put briefly, if a statically admissible stress field can be found such that yield is exceeded nowhere in the problem

* Corresponding author. Fax: +44-191-374-2550.
E-mail address: charles.augarde@dur.ac.uk (C.E. Augarde).

0266-352X/03/$ - see front matter
doi:10.1016/S0266-352X(03)00009-0

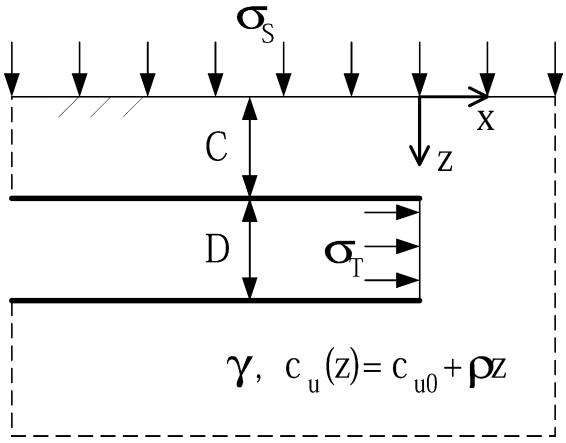

Fig. 1. Layout of plane strain heading problem.

region, then it is a safe solution (a *lower bound*) to the problem. Alternatively, an unsafe solution (an *upper bound*) can be found from a kinematically admissible collapse mechanism by equating internal power dissipated with external power expended. The bound theorems apply only to rigid-plastic materials. Were the object of this research the determination of deformations, rather than collapse conditions, then the displacement finite element method, using an elasto-plastic material model, would be appropriate. It is important to note, however, that the elastic parameters of any elasto-rigid plastic material model would not affect the solution for the collapse load [1].

Finite element implementations of the bound theorems were first proposed by Lysmer [2], for the lower bound case, and Anderheggen and Knopfel [3], for the upper bound case. Sloan and co-workers have since developed these methods and have used then to study a range of stability problems in geomechanics. Indeed, part of this paper updates an earlier study described in Sloan and Assadi [4] using recent developments in the solution algorithms of the finite element limit procedures to draw more accurate bounds on stability parameters. This paper also extends previous work into inhomogeneous soils.

The stability of underground openings in soft ground has been of interest to researchers since the late 1960's, although the literature on the subject is surprisingly sparse. A programme of (largely) experimental research at Cambridge was undertaken in the 1970's, culminating in the work of Mair [5] who used centrifuge testing to model two and three-dimensional models of tunnels in clay. Some of the results of Mair's study, and of other work from Cambridge at the time, are included in the paper by Davis et al. [6]. The latter also presents a range of solutions based on bound theorems, for unlined plane strain tunnels, circular headings as well as the plane strain heading. Some of these solutions are used below to check the numerical results.

The bound theorems have also been used to develop solutions for the stability of tunnels (but not plane strain headings) in drained conditions [7–9]. Very few researchers have attempted to use methods other than the bound theorems to study the stability of underground openings. Eisenstein and Samarasekara [10] examine the stability of tunnels in clay using a novel mix of limit equilibrium and displacement finite element results. Anagnostou and Kovari [11] also employ limit equilibrium methods to study pressures required for earth pressure balance tunnels in drained conditions. Neither of these approaches, however, provides the type of results furnished by bound approaches, which give safe and unsafe limits on stability parameters that bracket the true solution.

Where the bound theorems of plasticity have been used, in the works cited above, conventional analytical approaches (such as the Method of Characteristics) have been used. Since the late 1980's, Sloan and co-workers have developed finite element bound methods that are more versatile than conventional use of the bound theorems. These techniques, which are described in more detail below, permit inhomogeneous soil profiles and soil self-weight, two features that often prove difficult to incorporate in a conventional bound analysis. These methods have been used to study the undrained stability of square and circular unlined tunnels [12,13] as well as the plane strain heading [4]. They have also been used to predict the stability of a circular unlined tunnel in cohesive-frictional soil [14].

2. Problem definition

The layout of the plane strain heading stability problem is shown in Fig. 1. The heading has a height, D and cover C. The heading is lined with a smooth, rigid liner along its length. (It is important to stress again that this problem is not the same as a plane strain circular tunnel which represents an infinitely long unlined circular tunnel. The problem studied here is one of an infinitely long flat wall, of height D.) The presence of the liner implies the presence of reaction forces. These are however of no consequence in the numerical formulation adopted here as the liner is modelled as infinitely strong. The face of the heading is free to move and is subject to a normal stress representing an internal pressure σ_T. This pressure could be provided by compressed air. The ground surface is horizontal and subject to a vertical surcharge σ_s. For all analyses presented here, these stresses are taken as positive when directed into the heading face (σ_T) or vertically downwards (σ_s).

The ground around the excavation is modelled as a rigid plastic Tresca material with constant unit weight γ. This material has a single strength property, undrained shear strength, and is the same as the Mohr–Coulomb

criterion for the case of zero friction angle. The undrained shear strength of the soil in the analyses described here is permitted to vary linearly with depth, according to

$$c_u(z) = c_{u0} + \rho z \tag{1}$$

where c_{u0} is the undrained shear strength at the surface and ρ is the rate of change of shear strength with depth z from the surface (as indicated in Fig. 1). (Obviously, a homogeneous soil strength profile is modelled with $\rho = 0$). A linear variation of undrained shear strength with depth in normally consolidated (NC) clays has been observed empirically by Skempton [15] and is predicted by Critical State Soil Mechanics [16]. Skempton [15] proposes the following relation between undrained shear strength and plasticity index I_p

$$\frac{c_u(z)}{\sigma'_v(z)} = 0.11 + 0.0037 I_p \tag{2}$$

where σ'_v is the effective vertical stress. Ladd et al. [17] give the following expression for the undrained strength profile in an overconsolidated (OC) deposit

$$\frac{\left(c_u(z)/\sigma'_v(z)\right)_{OC}}{\left(c_u(z)/\sigma'_v(z)\right)_{NC}} = (OCR)^{0.8} \tag{3}$$

where OCR is the overconsolidation ratio. These relations are used to determine the range of values of the parameter ρ used in the parametric study presented later in the paper. The use of a simple rigid–plastic material model for the soil in this problem is necessary as the bound theorems of plasticity underlie the numerical procedures used in this paper.

3. Problem variables and dimensional analysis

Seven variables model instances of the plane strain heading problem outlined above, namely the group $\{\sigma_T, \sigma_s, C, D, c_{u0}, \gamma, \rho\}$. A convenient set of dimensionless groups that follows the requirements for dimensional analysis (usefully described in [18]) is the collection

$$\left\{\frac{\sigma_T}{c_{u0}}, \frac{\sigma_S}{c_{u0}}, \frac{\gamma D}{c_{u0}}, \frac{C}{D}, \frac{\rho D}{c_{u0}}\right\} \tag{4}$$

It is possible to replace the first two by a single group $(\sigma_S - \sigma_T)/c_{u0}$ because all calculations presented here assume undrained behaviour. To justify this reduction, it is necessary to consider the bound theorems individually. A statically admissible stress field satisfying the requirements of the lower bound theorem is also admissible for any addition of isotropic stress, since undrained strength is independent of total mean normal stress [6], (although such a combined stress field would not satisfy the stress boundary conditions in this problem). Therefore, only the difference between σ_S and σ_T needs to be considered. In the case of the upper bound theorem, the external power expended by the loads and the self-weight of the deforming soil mass is given by

$$P_{ext} = \sigma_S \int_{A_S} v_n^S \mathrm{d}A - \sigma_T \int_{A_T} v_n^T \mathrm{d}A + \gamma \int_V v \mathrm{d}V \tag{5}$$

where v_n^S is the downwards normal velocity at the surface, v_n^T is the outward normal velocity on the tunnel face and v is the vertical velocity of points within the soil mass. A_T and A_S are the deforming areas on the tunnel face and at the surface respectively. The last integral on the right hand side of Eq. (5) is taken over the soil volume V. Since undrained behaviour is assumed, the soil deforms at constant volume and

$$\int_{A_S} v_n^S \mathrm{d}A = \int_{A_T} v_n^T \mathrm{d}A \tag{6}$$

It is then possible to rewrite Eq. (5) in terms of the dimensionless groups given above as

$$P_{ext} = \left(\frac{\sigma_S - \sigma_T}{c_{u0}}\right) c_{u0} \int_{A_T} v_n^T \ \mathrm{d}A + \left(\frac{\gamma D}{c_{u0}}\right) \frac{c_{u0}}{D} \int_V v \mathrm{d}V \tag{7}$$

Engineers faced with a stability problem of this type are usually working with a given heading configuration and a soil profile determined from site investigation. In terms of the dimensionless groups given above, this can be restated as the determination of values of the parameter $(\sigma_S - \sigma_T)/c_{u0}$ given values of $\left\{\frac{\gamma D}{c_{u0}}, \frac{C}{D}, \frac{\rho D}{c_{u0}}\right\}$. In most practical situations the heading will be unpressurised ($\sigma_T = 0$), in which case the results from the stability analysis will be the surcharge load parameter σ_S/c_{u0}.

An alternative approach, adopted by many previous researchers, is to assess stability in terms of a "stability ratio" or overload factor (usually denoted N), by adding a term that represents an initial overburden stress to the load parameter $(\sigma_S - \sigma_T)/c_{u0}$. Broms and Bennermark [19] introduced this approach, giving the following definition for a homogeneous soil

$$N = \frac{\sigma_s - \sigma_T + \gamma(C + D/2)}{c_{u0}} \tag{8}$$

which is also adopted by Davis et al. [6] and Atkinson and Mair [20], although the latter rename the parameter, T_c. This approach appears to be a way of reducing the complexity of the final results. It does, however, lead to problems as $(\sigma_S - \sigma_T)/c_{u0}$ itself depends on the parameter $(\gamma D)/c_{u0}$. (This will be demonstrated from first principles for the case of an upper bound solution later in the paper). Additionally, it is not clear what is an appropriate choice for the shear strength denominator in Eq. (8) for an inhomogeneous soil. Given these difficulties, the results from the analyses described in this paper are presented in terms of the load parameter

$(\sigma_S - \sigma_T)/c_{u0}$. This approach follows both the requirements of dimensional analysis and of rigorous plasticity theory.

4. Finite element formulation of the bound theorems

The finite element formulations of the bound theorems, as developed by Sloan for use in geomechanics problems, are described in detail in a number of references (e.g. [12,21]). Only a brief description of the procedures is therefore given here, and the reader is referred to the original publications for full details of the formulations. It is important to note that the formulations are not variations of the displacement finite element method, but employ the same idea of discretisations of a domain to obtain solutions.

The lower bound theorem requires a statically admissible stress field that obeys the yield criterion throughout the problem domain. Conventional analytical approaches seek to divide the domain into regions in which statically admissible stress fields are defined. Between regions, discontinuities in the normal stresses in the direction of the discontinuity are permitted. These allow the stress boundary conditions for the problem to be satisfied (for applied loads and prescribed displacements). The finite element formulation of the lower bound theorem has the same goal but the regions are replaced by three-noded triangular finite elements within which stress fields can vary linearly. The nodal variables associated with each element are the stresses at the nodes. While elements are notionally connected at nodes, the nodal stresses are associated with that element only, unlike displacement finite elements. Stress discontinuities are permitted between each element in the domain. Special ''extension'' elements are also placed on the boundary to model an unbounded domain, and hence produce a rigorous lower bound. The calculation then proceeds as an optimisation of the domain stress field, where the constraints are those imposed by equilibrium, the stress boundary conditions and the yield criterion. The objective function, to be maximized, is the integral of the normal stresses over some part of the domain. (For the case of the plane strain heading, this is difference between the surcharge σ_S and the tunnel pressure σ_T). The Tresca yield criterion leads to a set of non-linear constraints on the nodal stresses. To form a linear programming problem, this non-linearity is dealt with by replacement of the non-linear constraints with linear inequalities that maintain a rigorous lower bound solution [4,21]. This can be visualised as replacing the circular Tresca surface (in Cartesian stress space) with an n-sided internal prism.

The procedure outlined above has proved successful for many two-dimensional problems. The process of linearising the yield surface for very large (i.e. finely discretised) two-dimensional problems leads, however, to an excessive number of linear inequalities. The linear programming problem that is produced is consequently slow to solve using traditional methods (such as the simplex method).

An alternative approach has been developed recently where the yield function is left non-linear and the problem is recast as a non-linear programming problem [22,23] to

$$\begin{aligned} &\text{Maximise} && \mathbf{c}^{\mathrm{T}}\boldsymbol{\sigma} \\ &\text{Subject to} && \mathbf{A}\boldsymbol{\sigma} = \mathbf{b} \\ & && f_i(\boldsymbol{\sigma}) \leqslant 0 \quad i = \{1, \ldots, N\} \end{aligned} \tag{9}$$

where $\boldsymbol{\sigma}$ is the vector of nodal stresses, $\mathbf{c}$ is a vector of objective function coefficients to transform the stresses to the optimised load, $\mathbf{A}$ and $\mathbf{b}$ are a matrix and vector respectively, of equality constraint coefficients derived from equilibrium and the stress boundary conditions, f_i is the yield function for node i and N is the number of nodes. The algorithm used to solve this system is described in detail in Lyamin and Sloan [23] and will not be repeated here. Recasting the problem in non-linear form, as described above, leads to a much faster solution. Early use of the formulation has indicated a 50-fold reduction in CPU time, as compared to the linear programming approach [22]. This gain in efficiency allows much larger two-dimensional problems to be solved and is the technique used to obtain the lower bound results presented later in this paper.

A similar finite element approach can be taken with the upper bound theorem. A conventional upper bound analysis proceeds by seeking a collapse mechanism that is kinematically admissible. This is a velocity field covering the domain that satisfies the velocity boundary conditions, and the plasticity flow rule (which is associated in the case of the Tresca criterion). For problems such as the plane strain heading, a mechanism may consist of rigid blocks of soil, moving at differing velocities. Internally, power is dissipated in the discontinuities between the blocks. This power is equated to the external power expended by the external loads (σ_T and σ_S) and the self-weight of the soil γ, to obtain an upper bound solution.

The original formulation of the upper bound theorem [24] proceeds similarly to the lower bound formulation, with rigid regions replaced by three-noded triangular elements over which the velocity is allowed to vary linearly. Each node has two unknown velocities specific to that element. Velocity discontinuities are permitted at specified locations in the finite element mesh, for which the sign of shearing must be specified by the analyst. Unlike a rigid-block mechanism approach, internal power may also be dissipated in plastic deformation of the continuum. To ensure kinematic admissibility, each

element therefore also has a specified number of plastic multiplier rates to ensure plastic deformation obeys the flow rule for the yield criterion used. The formulation also ensures that zero deformation occurs in regions where computed stresses lie within the yield surface. An optimisation problem then evolves with the objective function (to be minimized) being the internal power dissipation. The constraints arise from the need to satisfy kinematic admissibility (for continuous velocity fields between discontinuities, the plastic flow rule and velocity boundary conditions). In a similar fashion to the lower bound formulation, the problem can be solved by linear programming methods, by making the yield surface linear in Cartesian stress space.

The original formulation has a number of shortcomings that have been addressed in recent years. Firstly, the need to define the location and nature of velocity discontinuities a priori has been removed by techniques described in Sloan and Kleeman [25] with a novel formulation that permits velocity discontinuities along every element edge in the mesh. This has also removed the need to adopt fixed element patterns to ensure incompressible material behaviour.

More recently, Lyamin and Sloan [26] have developed an upper bound finite element formulation based on non-linear programming. The new finite element formulation of the upper bound theorem uses the same linear velocity elements as in the original formulation. Unlike the original formulation, however, each element is associated with a constant stress field and a single plastic multiplier rate, as the yield surface is not linearised in this formulation. The optimisation problem can then be cast in terms of the nodal velocities and the element stresses. Once again, the solution algorithm used for this non-linear programming problem is fully described elsewhere [26] and will not be repeated here. The new procedure is much quicker than the original linear programming formulation, permitting very fine discretisation for two-dimensional problems.

A previous study of the stability of a plane strain heading [4] was restricted to the linear programming approach of both lower and upper bound finite element formulations. The new techniques employed here have allowed much finer two-dimensional finite element meshes to be used, thus improving the quality of bound solutions.

5. Numerical results

The results of over four hundred finite element bound analyses of the plane strain heading problem, using the methods outlined above, are presented in Table 1. The results are also presented as dimensionless stability charts in Figs. 2–6. In all analyses, the load parameter $(\sigma_S - \sigma_T)/c_{u0}$ is optimised for set values of the other parameters in the group [Eq. (4)]. For both upper and lower bound analyses, the optimum value of the load parameter is found by setting σ_S to zero and optimising for σ_T alone. For the upper bound a uniform tunnel pressure is optimised by imposing the loading condition at the tunnel face equivalent to

$$\int_{A_T} v_n^T \mathrm{d}A = 1 \tag{10}$$

This does not restrict the upper bound solution to have a constant velocity profile over the heading height, an aspect of the finite element upper bound solutions which will be shown to have important consequences for the use of stability ratios, such as the one expressed in Eq. (8).

Results are presented for values of the weight parameter $(\gamma D)/c_{u0}$ of 0, 1, 2 and 3 and for five values of the strength inhomogeneity parameter $(\rho D)/c_{u0}$ between zero and unity. These values are chosen to cover a wide range of normally consolidated and overconsolidated soil conditions, following the relations given in Eqs. (2) and (3).

A typical mesh used to analyse a plane strain heading with $C/D = 2$ is shown in Fig. 7. Similar meshes are used for upper and lower bound analyses as the new formulation, based on non-linear programming, allows the use of a very large number of two-dimensional elements. It is therefore not necessary to experiment with a range of meshes to arrive at narrow bounds. The mesh shown in Fig. 7 has 27 936 nodes and 9312 triangular elements. The stress boundary conditions (for the lower bound analyses) ensure zero shear and normal stress at the surface, zero shear stress on the heading face and along the lined section of the heading. Extension elements are also included along the soil domain boundaries for the lower bound analyses. An upper bound analysis using the mesh in Fig. 7 includes velocity boundary conditions to ensure zero velocity at the boundaries, and zero vertical velocity along the lined section of the heading. As indicated in the description of the upper bound formulation, velocity discontinuities are present between each element in the mesh.

All results presented here were obtained using an AMD Athlon processor running at 1200 MHz and generally required between 40 and 480 CPU seconds per analysis. These timings are impressive given the complexity of the finite element meshes used in the analyses, and demonstrate the efficiency of the non-linear programming approach.

6. Analytical comparisons

It is important to check the results of any numerical model using existing analytical solutions where these are available. In this case, the main source of useful analy-

Table 1
Bounds on the load parameter for stability of an undrained plane strain heading

$\frac{C}{D}$	$\frac{\rho D}{c_{u0}}$	$\frac{\gamma D}{c_{u0}} = 0$		$\frac{\gamma D}{c_{u0}} = 1$		$\frac{\gamma D}{c_{u0}} = 2$		$\frac{\gamma D}{c_{u0}} = 3$	
		Lower bound	Upper bound	Lower bound	Upper bound	Lower bound	Upper bound	Lower bound	Upper bound
1	0.00	4.00	4.39	2.46	2.89	0.85	1.39	−0.74	−0.11
1	0.25	5.32	5.59	3.82	4.09	2.29	2.59	0.68	1.09
1	0.50	6.47	6.77	4.98	5.27	3.46	3.77	1.87	2.27
1	0.75	7.60	7.93	6.12	6.43	4.62	4.93	3.04	3.43
1	1.00	8.73	9.09	7.25	7.59	5.76	6.09	4.19	4.59
2	0.00	5.05	5.68	2.40	3.18	−0.20	0.68	−2.84	−1.82
2	0.25	7.93	8.10	5.43	5.60	2.91	3.08	0.37	0.54
2	0.50	10.42	10.66	7.93	8.17	5.43	5.66	2.90	3.14
2	0.75	12.89	13.19	10.41	10.71	7.91	8.21	5.40	5.70
2	1.00	15.35	15.72	12.87	13.24	10.38	10.74	7.87	8.24
3	0.00	5.75	6.50	2.20	3.00	−1.40	−0.50	−5.03	−4.00
3	0.25	10.20	10.50	6.70	7.00	3.19	3.48	−0.35	−0.05
3	0.50	14.23	14.66	10.74	11.16	7.24	7.66	3.72	4.14
3	0.75	18.23	18.79	14.75	15.30	11.25	11.80	7.75	8.30
3	1.00	22.22	22.91	18.74	19.42	15.25	15.93	11.75	12.43
4	0.00	6.25	7.21	1.71	2.71	−2.86	−1.79	−7.49	−6.29
4	0.25	12.52	12.82	8.03	8.32	3.52	3.81	−1.01	−0.72
4	0.50	18.28	18.72	13.79	14.23	9.29	9.72	4.78	5.21
4	0.75	24.01	24.59	19.52	20.10	15.03	15.60	10.53	11.09
4	1.00	29.72	30.45	25.24	26.00	20.75	21.46	16.25	16.96
5	0.00	6.70	7.70	1.15	2.20	−4.48	−3.30	−10.11	−8.80
5	0.25	14.81	15.19	9.32	9.69	3.81	4.18	−1.71	−1.35
5	0.50	22.40	22.98	16.92	17.48	11.42	11.98	5.91	6.47
5	0.75	29.96	30.72	24.48	25.23	18.99	19.73	13.49	14.23
5	1.00	37.51	38.46	32.03	32.97	26.54	27.47	21.05	21.97
6	0.00	7.02	8.12	0.41	1.62	−6.10	−4.88	−12.90	−11.38
6	0.25	17.14	17.58	10.65	11.08	4.14	4.57	−2.39	−1.95
6	0.50	26.67	27.36	20.18	20.87	13.69	14.36	7.18	7.86
6	0.75	36.17	37.11	26.69	30.61	23.20	24.11	16.70	17.61
6	1.00	45.66	46.84	39.17	40.34	32.69	33.85	26.19	27.35
7	0.00	7.33	8.49	−0.32	0.99	−7.90	−6.51	−15.53	−14.01
7	0.25	19.47	20.02	11.98	12.50	4.47	5.00	−3.05	−2.52
7	0.50	31.01	31.87	23.53	24.37	16.03	16.87	8.53	9.36
7	0.75	42.53	43.70	35.04	36.20	27.55	28.71	20.06	21.21
7	1.00	54.02	55.51	46.54	48.02	39.06	40.53	31.56	33.03
8	0.00	7.46	8.83	−1.21	0.33	−9.80	−8.17	−18.43	−16.67
8	0.25	21.82	22.46	13.33	13.96	4.82	5.45	−3.70	−3.06
8	0.50	35.44	36.49	26.95	27.99	18.46	19.49	9.96	10.99
8	0.75	49.02	50.48	40.55	41.99	32.06	33.49	23.56	24.99
8	1.00	62.60	64.46	54.12	55.97	45.64	47.47	37.14	38.97
9	0.00	7.57	9.08	−2.16	−0.42	−11.75	−9.92	−21.39	−19.42
9	0.25	24.19	24.95	14.70	15.46	5.19	5.95	−4.33	−3.57
9	0.50	39.94	41.21	30.46	31.72	20.96	22.22	11.46	12.71
9	0.75	55.66	57.43	46.17	47.94	36.68	38.44	27.19	28.94
9	1.00	71.37	73.64	61.88	64.15	52.40	54.65	42.90	45.16
10	0.00	7.70	9.32	−3.16	−1.18	−13.75	−11.68	−24.39	−22.18
10	0.25	29.58	27.48	16.09	16.98	5.58	6.48	−4.94	−4.03
10	0.50	44.51	46.03	34.02	35.54	23.52	25.04	13.02	14.53
10	0.75	62.40	64.54	51.92	54.05	41.43	43.55	30.93	33.06
10	1.00	80.29	83.06	69.80	72.56	59.32	62.06	48.82	51.57

tical checks on the numerical results comes from Ref. [6]. They present analytical solutions for lower and upper bounds of the load parameter $(\sigma_S - \sigma_T)/c_{u0}$ for undrained soil with constant strength with depth. For the case of a weightless soil $(\gamma D)/c_{u0} = 0$, a lower bound can be obtained by adapting the solution for a v-notched bar under tension, given in [27]

$$\frac{\sigma_S - \sigma_T}{c_{u0}} \geqslant 2 + 2\log\left(\frac{C}{D} + 1\right) \tag{11}$$

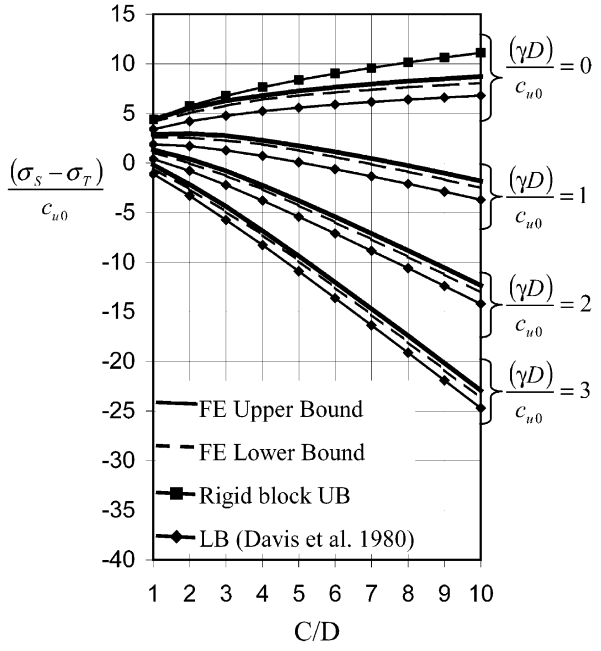

Fig. 2. Bounds on load parameter for $(\rho D)/c_{u0} = 0$.

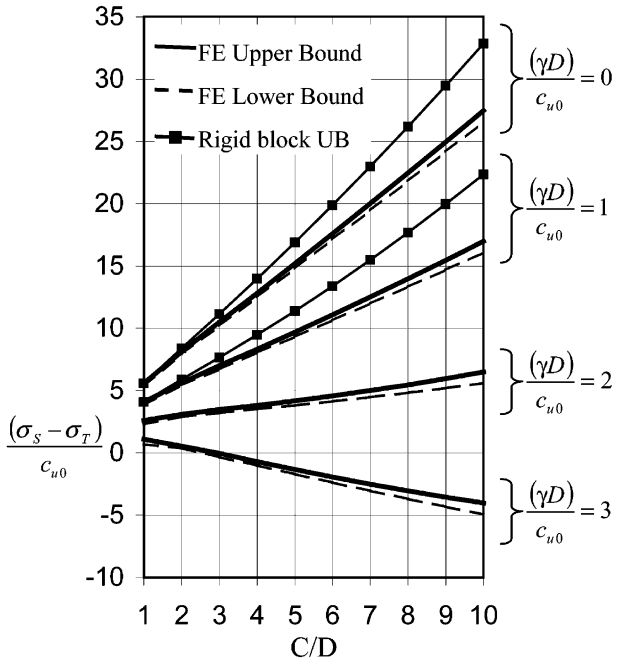

Fig. 3. Bounds on load parameter for $(\rho D)/c_{u0} = 0.25$.

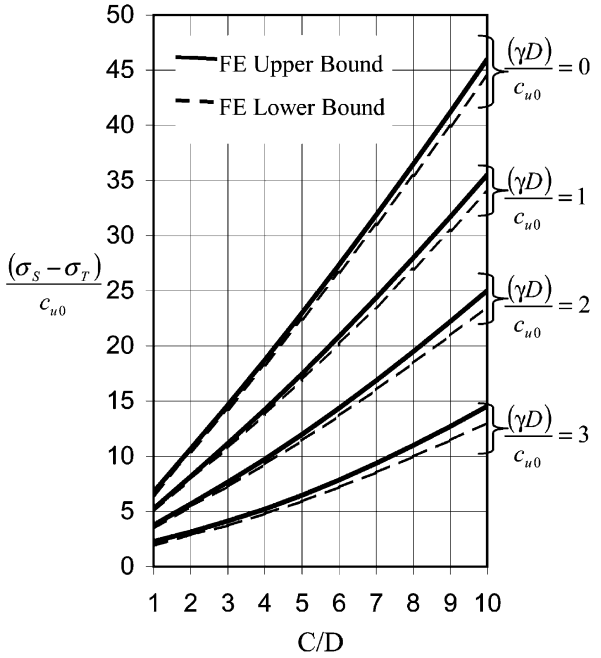

Fig. 4. Bounds on load parameter for $(\rho D)/c_{u0} = 0.5$.

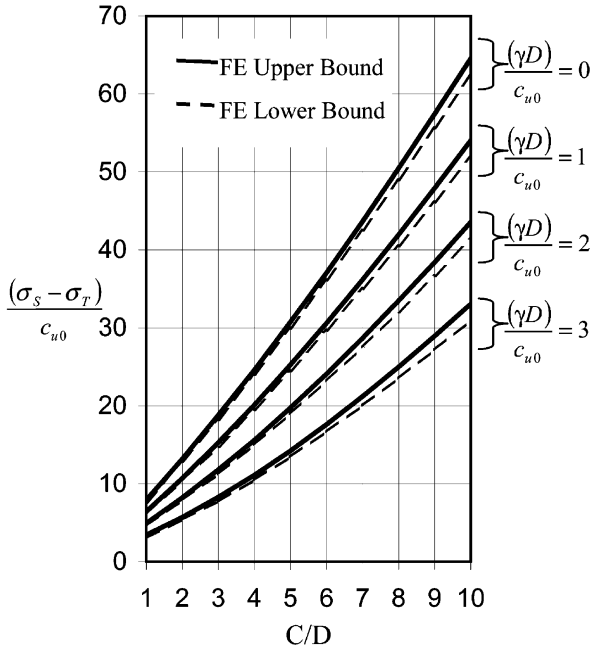

Fig. 5. Bounds on load parameter for $(\rho D)/c_{u0} = 0.75$.

For the case of a soil with self-weight, $(\gamma D)/c_{u0} \neq 0$, Davis et al. [6] suggest it is acceptable to add a hydrostatic stress field to the weightless case to obtain a solution. This is not a strict lower bound, as the tunnel pressure now varies linearly with depth, rather than being constant over the depth; the condition used to derive the original weightless lower bound solution. If σ_T is taken instead to represent the mean tunnel pressure over the heading height then this solution can be written

$$\frac{\sigma_S - \sigma_T}{c_{u0}} \geqslant 2 + 2\log\left(\frac{C}{D}+1\right) - \frac{\gamma D}{c_{u0}}\left(\frac{C}{D}+\frac{1}{2}\right) \tag{12}$$

Davis et al. [6] suggest this is, however, a safe solution based on their results for the other stability problems. These lower bound solutions are by inspection, also lower bound solutions for the case of inhomogeneous soil, albeit very poor ones.

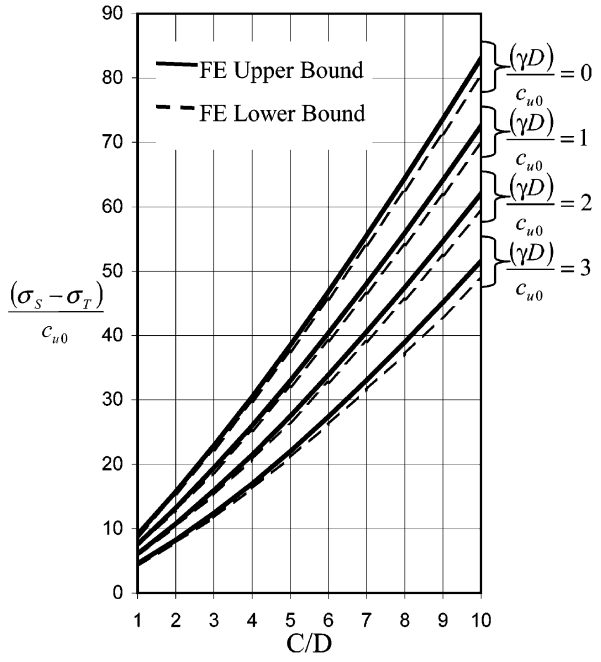

Fig. 6. Bounds on load parameter for $(\rho D)/c_{u0} = 1.0$.

An analytical upper bound solution can be obtained from the five variable mechanism shown in Fig. 8 [4]. This is a rigid block mechanism where the internal power dissipation takes place along the interfaces between blocks only. The mechanism may appear to be incompatible in that the tip of the triangle at the face of the heading has to penetrate the soil beneath. This difficulty is dealt with by noting that if the tip deforms plastically to accommodate this movement the energy dissipated is of second order to that dissipated in the interfaces between blocks for a given movement, and can be neglected in the analysis [28]. Similar mechanisms are also used by Davis et al. [6]. For the case of a constant undrained strength $(\rho D)/c_{u0} = 0$, equating external and internal power dissipation and rearranging gives the following expression for the load parameter,

$$\left.\frac{\sigma_S - \sigma_T}{c_{u0}}\right|_{\frac{\rho D}{c_{u0}}=0} =$$

$$\frac{2C}{D}\left[\frac{\sin\theta_2\sin\theta_4}{\sin\theta_1\sin\theta_3\sin\theta_5\cos(\theta_1+\theta_2+\theta_3+\theta_4+\theta_5)}\right]$$

$$+\cot\theta_1+2\cot\theta_2+2\cot\theta_3+2\cot\theta_4+\cot\theta_5$$

$$+\frac{\cos(\theta_1+\theta_2+\theta_3+\theta_4)}{\sin\theta_5\cos(\theta_1+\theta_2+\theta_3+\theta_4+\theta_5)}-\frac{\gamma D}{c_{u0}}\left[\frac{C}{D}+\frac{1}{2}\right] \quad (13)$$

This mechanism can also be used for the case of varying soil strength with depth, in which case the expression for the load parameter is

$$\left.\frac{\sigma_S - \sigma_T}{c_{u0}}\right|_{\frac{\rho D}{c_{u0}}\neq 0} = \left.\frac{\sigma_S - \sigma_T}{c_{u0}}\right|_{\frac{\rho D}{c_{u0}}=0} + \frac{\rho D}{c_{u0}}$$

$$\left[\frac{C}{D}\left(\begin{array}{l}\cot\theta_1+2\cot\theta_2+2\cot\theta_3+2\cot\theta_4+\cot\theta_5\\ +\dfrac{\cos(\theta_1+\theta_2+\theta_3+\theta_4)}{\sin\theta_5\cos(\theta_1+\theta_2+\theta_3+\theta_4+\theta_5)}\end{array}\right)+\left(\frac{C}{D}\right)^2\right.$$

$$\left(\frac{\sin\theta_2\sin\theta_4}{\sin\theta_1\sin\theta_3\sin\theta_5\cos(\theta_1+\theta_2+\theta_3+\theta_4+\theta_5)}\right)$$

$$+\frac{1}{2\sin\theta_2}\left(\begin{array}{l}\dfrac{\sin(\theta_1+\theta_2)}{\sin\theta_1}-\cos(\theta_1+\theta_2)\\ (\cos\theta_1+\sin\theta_1(2\cot\theta_2+2\cot\theta_3+\cot\theta_4))\end{array}\right)$$

$$\left.+\frac{1}{2\sin\theta_2}\left(\begin{array}{l}\dfrac{\cos(\theta_1+\theta_2+\theta_3+\theta_4)}{\sin\theta_4}(\sin\theta_3(\cot\theta_4+\cot\theta_5))\\ +\dfrac{\sin\theta_3\cos(\theta_1+\theta_2+\theta_3+\theta_4)}{\sin\theta_5\cos(\theta_1+\theta_2+\theta_3+\theta_4+\theta_5)}\\ +\dfrac{\sin(\theta_3+\theta_4)}{\sin\theta_4}\end{array}\right)\right] \quad (14)$$

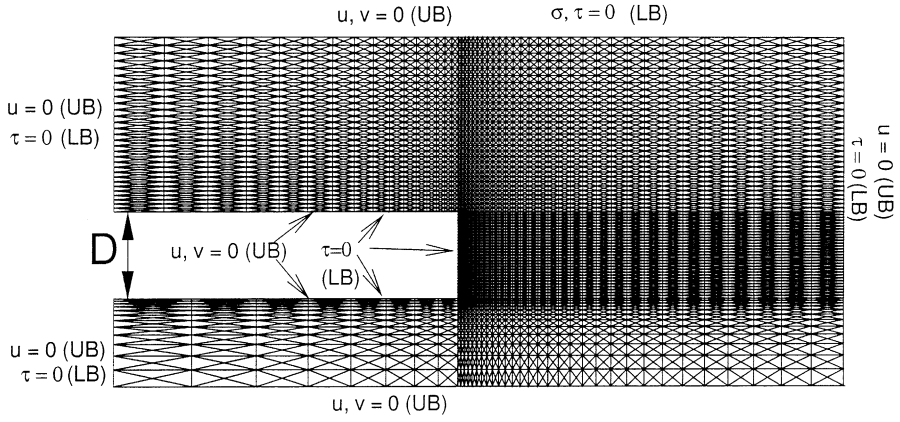

Fig. 7. Typical finite element mesh for C/D = 2.

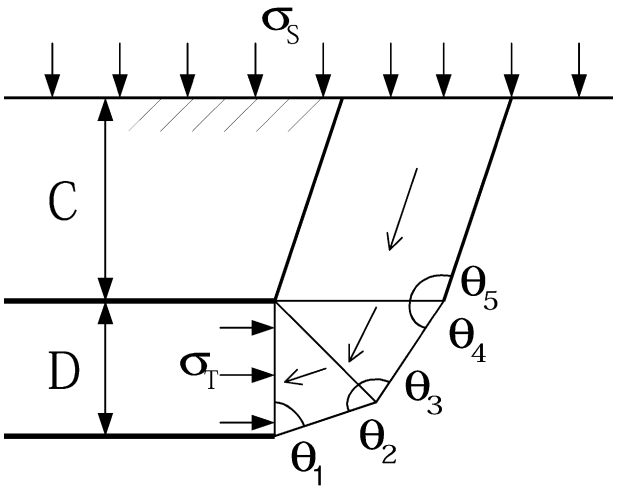

Fig. 8. 5-variable rigid block mechanism for analytical upper bound.

Upper bounds can then be found by numerically optimising Eqs. (13) and (14). Values thus obtained are included, where appropriate, with the plots of the finite element results, in Figs. 2–6. A limited number of cases only, for the analytical solutions given above, are included in these figures, because the finite element results usually provide much better bounds and also for the sake of clarity.

It is notable that upper bound solutions for soils where $\gamma D/c_{u0} > 0$ can be derived from the weightless solutions by subtraction of a term including two of the dimensionless groups.

This apparently convenient result was derived independently for any upper bound solution of this problem by Sloan and Assadi [4]. It appears to make the use of a stability ratio N, as defined in Eq. (8), rather attractive as the term deducted from the upper bound solutions for $\gamma D/c_{u0} > 0$ is equal to the term added to the load parameter to obtain N. One stability parameter therefore covers all cases of soil with and without self-weight, for a particular configuration of heading. This is applicable only in certain cases, however, as will be demonstrated below.

The external power term required for the upper bound analysis [Eq. (7)] includes an integral of the vertical velocity v of points in the soil mass. Due to the incompressibility of the soil it is possible to replace this integral with a simpler term that can be evaluated in terms of the geometry of the problem and the nature of the horizontal velocity profile applied to the tunnel face as follows:

$$\int_V v \, \mathrm{d}V = \int_C^{C+D} z v_n^T \, \mathrm{d}z \tag{15}$$

where v_n^T is the horizontal outward velocity at the face of the heading (as before) and z is the vertical coordinate, as shown in Fig. 1. [A detailed proof of the derivation of Eq. (15) is given by Sloan and Assadi [4]]. If a uniform outward velocity field $v_n^T = \delta$ is imposed on the heading face then, using Eq. (15) the volume integral in Eq. (7) is

$$\int_V v \, \mathrm{d}V = \delta D\left(C + \frac{D}{2}\right) \tag{16}$$

Substituting this result into the expression for the external power expended [Eq. (7)] and equating to the internal power, P_{int} gives

$$P_{int} = \left(\frac{\sigma_S - \sigma_T}{c_{u0}}\right) c_{u0}\delta D + \left(\frac{\gamma D}{c_{u0}}\right) c_{u0}\delta D\left(C + \frac{D}{2}\right) \tag{17}$$

Hence we can write the result for soil with self-weight in terms of the solution for the weightless soil as

$$\left(\frac{\sigma_S - \sigma_T}{c_{u0}}\right)_{\frac{\gamma D}{c_{u0}} \neq 0} = \left(\frac{\sigma_S - \sigma_T}{c_{u0}}\right)_{\frac{\gamma D}{c_{u0}} = 0} - \left(\frac{\gamma D}{c_{u0}}\right)\left(\frac{C}{D} + \frac{1}{2}\right) \tag{18}$$

This is similar in form to the upper bound solutions using the rigid block mechanism in Fig. 8 [Eqs. (13) and (14)]. As is now evident, however, the second term in Eq. (18) changes according to the chosen velocity distribution on the heading face. If, for example, the velocity v_n^T varies linearly from δ at the top of the heading to zero at the base, as shown in Fig. 9, the second term on the right hand side of Eq. (18) becomes $\left(\frac{\gamma D}{c_{u0}}\right)\left(\frac{C}{D} + \frac{1}{3}\right)$.

7. Discussion

The numerical results presented in Figs. 2–6 show very close bounds on the load parameter $(\sigma_S - \sigma_T)/c_{u0}$ for a wide range of problem configurations. The closeness of the bounds, and the feasibility of conducting such a large study, can be attributed to the improve-

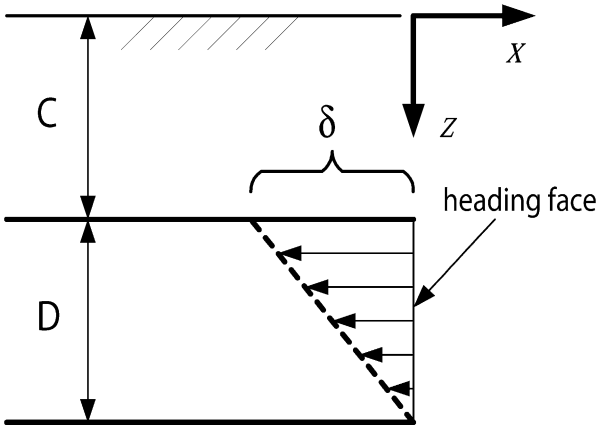

Fig. 9. Linear variation of velocity over heading depth.

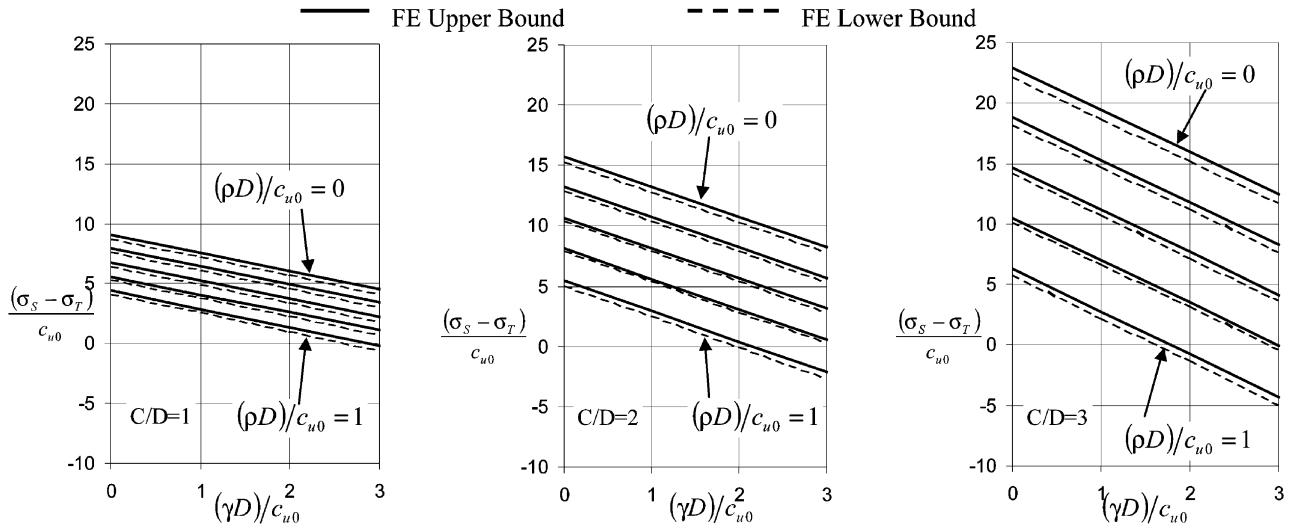

Fig. 10. Load parameters replotted for varying weight parameter.

ments in the algorithms used to solve the non-linear programming problem, resulting from the finite element bound formulation. In the majority of cases the bound solutions bracket the real solution to within ±4%. As the soil weight parameter $\gamma D/c_{u0}$ is increased, the gap between the bounds widens slightly, as does the calculation time to obtain the results.

A negative value of the load parameter $(\sigma_S - \sigma_T)/c_{u0}$ indicates the heading configuration is inherently unstable; i.e. a positive heading pressure is required to prevent collapse, with zero surcharge. This situation occurs for a limited range of headings, generally for heavy soils, with $(\gamma D)/c_{u0} \geqslant 2$ where there is little or no increase of strength with depth. For all cases where there is appreciable inhomogeneity [with$(\rho D)/c_{u0} \geqslant 0.5$], all headings are stable for zero surcharge and zero heading pressure.

The analytical and rigid-block bound solutions [Eqs. (11)–(14)] improve on the finite element results for one case only ($C/D = 2$, $\gamma D/c_{u0} = \rho D/c_{u0} = 0$) and in general provide much poorer solutions. For shallow headings with low soil weight, however, the analytical upper bound solutions [Eqs. (13) and (14)] are very close to those given by the finite element methods. The lower bound solution for soils with self-weight, suggested by Davis et al. [6] are indeed safe, as can be seen in Fig. 2. This solution also appears to follow the same trend as the finite element lower bound solutions.

Another noticeable feature of the results is the relative importance of soil weight and strength profile. As the latter is increased from 0.5 to unity, the importance of the soil weight profile decreases considerably. When $(\rho D)/c_{u0} = 0.5$, the load parameter is reduced three-fold as the weight parameter changes from zero to 3. For the steepest increase in strength with depth $(\rho D)/c_{u0} = 1.0$, the load parameter for weightless soils conditions is only 1.6 times that at the highest weight parameter. The opposite effect happens when the heading is located at a greater depth. Fig. 10 shows the variations in the load parameter as weight increases, from $C/D = 1$ to $C/D = 3$. The plots for the shallow heading are closely spaced, in contrast to those for the deeper heading. This confirms, perhaps obviously, that the determination of the variable ρ assumes greater importance as the heading depth increases.

Fig. 10 also shows a linear variation in load parameter with weight parameter, for both upper and lower bound results. This follows the predictions from the analytical upper bound solutions discussed above, where solutions for soils with self-weight are found by subtracting a term dependent on $\gamma D/c_{u0}$ from the weightless load parameter.

Fig. 11a shows the velocity vectors at nodes in an upper bound mesh for a heading where $C/D = 1$, $\gamma D/c_{u0} = 3$, $\rho D/c_{u0} = 0$. Horizontal components at the tunnel face (i.e. values of v_n^T) are clearly non-uniform over the tunnel height. In this case, therefore, the stability number given in Eq. (8) would not be valid. This demonstrates that the safe use of a stability number, N, requires prior knowledge of the velocity profile over the heading height. Similar conclusions may be drawn for other underground stability problems in geomechanics. Non-uniform horizontal velocity profiles at the heading face, obtained in the finite element solutions, are shown to produce better upper bound solutions and to invalidate the use of the stability ratio as described by Eq. (8). There are also interesting differences in the patterns of these velocities as soil weight increases and as headings are deepened. The effect of increasing soil weight is to make the velo-

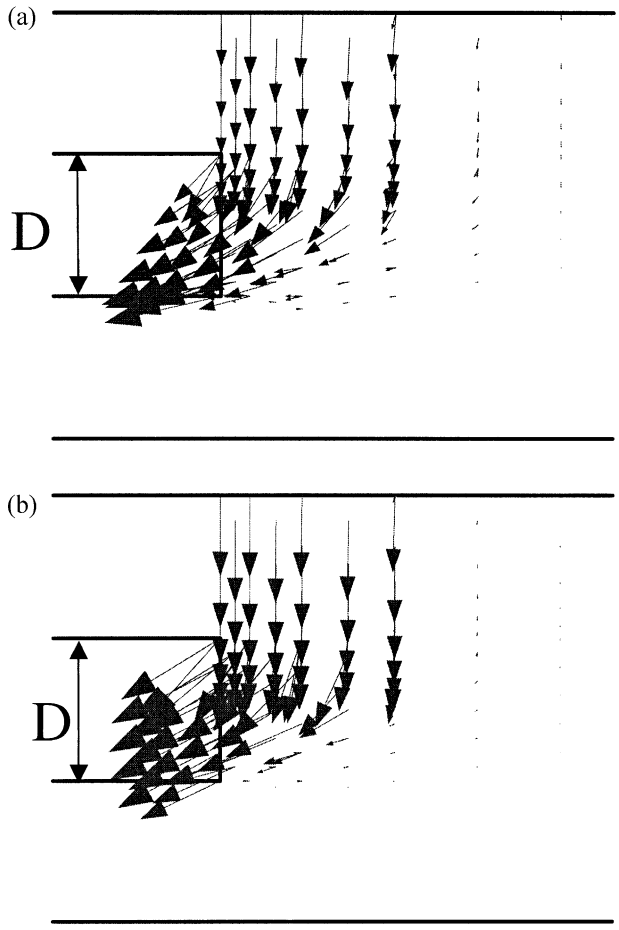

Fig. 11. Velocity vectors for finite element upper bound analyses $C/D = 1$, $\rho D/c_{u0} = 0$: (a) $\gamma D/c_{u0} = 0$, (b) $\gamma D/c_{u0} = 3$.

city profile over the heading depth less uniform. Fig. 11b shows the profile for $C/D = 1$, $\gamma D/c_{u0} = 0$, $\rho D/c_{u0} = 0$ and indicates relatively uniform velocity vectors over the heading depth. Fig 10a, in contrast shows the velocity vectors for the same analysis with $\gamma D/c_{u0} = 3$. The profile, as highlighted above, is clearly less uniform with greater velocities to the base of the heading and reduced velocities at the top. This pattern is evident for all depths of heading studied here. Fig. 12a and b show a similar effect for the case where $C/D = 5$. Clearly, increased soil weight leads to a larger variation in vertical stress across the heading and this may lead to earlier yield and a greater contribution to continuum plastic flow in the base of the heading. Fig. 12 also shows the finite element upper bound to depart from the rigid block mechanism of Fig. 8 once the heading is at depth. Non-zero velocities are predicted for nodes above the lined section of the tunnel for this case, $C/D = 5$, and deeper cases. For the case of $C/D = 1$, velocity discontinuities appears to line up vertically from the top of the heading, similar to the rigid block mechanism of Fig. 8.

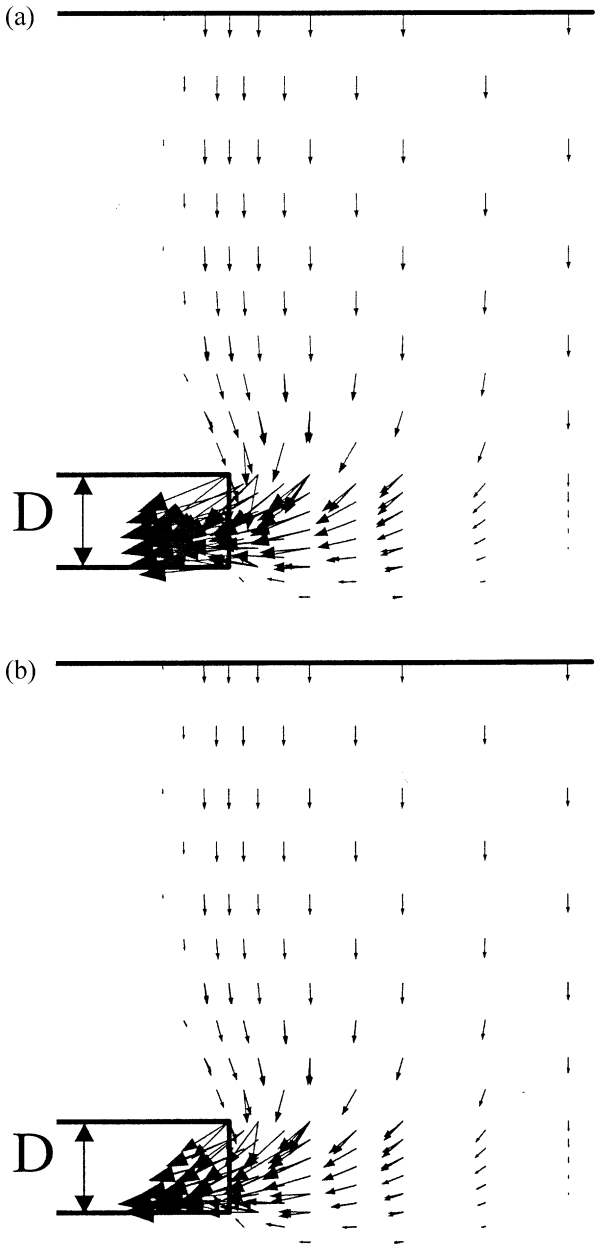

Fig. 12. Velocity vectors for finite element upper bound analyses $C/D = 5$, $\rho D/c_{u0} = 0$: (a) $\gamma D/c_{u0} = 0$, (b) $\gamma D/c_{u0} = 3$.

8. Conclusion

The stability of a plane strain heading in undrained conditions has been investigated using finite element bound methods. Improvements to solution algorithms have permitted very close bounds to be drawn in most cases, providing useful charts for those assessing the stability of this type of underground opening. It is important to remember that, in practice, the drained stability should also be considered, an area not covered in this paper. The use of a universal stability ratio [19] has been shown not to be advisable, depending as it does on the nature of collapse which cannot be determined a priori.

Acknowledgements

The work presented in this paper was carried out while the first author was visiting the University of Newcastle, Australia. During this period he was supported by an IREX Fellowship, awarded by the Australian Research Council.

References

[1] Salencon J. An introduction to the yield design theory and its application to soil mechanics. European Journal of Mechanics A/Solids 1990;9(5):477–500.
[2] Lysmer J. Limit analysis of plane problems in soil mechanics. ASCE Journal of the Soil Mechanics and Foundations Division 1970;96(SM4):1311–34.
[3] Anderheggen E, Knopfel H. Finite element limit analysis using linear programming. International Journal of Solids and Structures 1972;8:1413–31.
[4] Sloan SW, Assadi A. Undrained stability of a plane strain heading. Canadian Geotechnical Journal 1994;31:443–50.
[5] Mair, RJ. Centrifugal modelling of tunnel construction in soft clay. PhD thesis, University of Cambridge, 1979.
[6] Davis EH, Gunn MJ, Mair RJ, Seneviratne HN. The stability of shallow tunnels and underground openings in cohesive material. Géotechnique 1980;30:397–416.
[7] Mühlhaus H-B. Lower bound solutions for tunnels in two and three dimensions. Rock Mechanics and Rock Engineering 1985; 18:37–52.
[8] Atkinson JH, Potts DM. Stability of a shallow circular tunnel in cohesionless soil. Géotechnique 1977;27:203–15.
[9] Leca E, Dormieux L. Upper and lower bound solutions for the face stability of shallow circular tunnels in frictional material. Géotechnique 1990;40:581–606.
[10] Eisenstein Z, Samarasekara L. Stability of unsupported tunnels in clay. Canadian Geotechnical Journal 1992;29:609–13.
[11] Anagnostou G, Kovari K. Face stability conditions with earth-pressure-balanced shields. Tunnelling and Underground Space Technology 1996;11:165–73.
[12] Sloan SW, Assadi A. Undrained stability of a square tunnel whose strength increases linearly with depth. Computers and Geotechnics 1991;12:321–46.
[13] Sloan SW, Assadi A. The stability of tunnels in soft ground. In: Houlsby GT, Schofield AN, editors. Predictive soil mechanics. London: Thomas Telford 1993, p. 644–63.
[14] Lyamin AV, Sloan SW. Stability of a plane strain circular tunnel in a cohesive-frictional soil. In: Proceedings of the J.R. Booker Memorial Symposium, Sydney, 2000. p. 139–53.
[15] Skempton AW. The planning and design of the new Hong Kong airport. Discussion. Proc Inst Civil Eng 1957;7:305–7.
[16] Atkinson JH, Bransby PL. The mechanics of soils: an introduction to critical state soil mechanics. London: McGraw-Hill; 1978.
[17] Ladd CC, Foote R., Ishihara K, Schlosser F, Poulos HG. Stress deformation and strength characteristics. In: Proc. 12th Int. Conf. Soil Mechanics and Foundation Engineering, Vol. 2, 1977. p. 421–94.
[18] Butterfield R. Dimensional analysis for geotechnical engineers. Géotechnique 1999;49:357–66.
[19] Broms BB, Bennermark H. Stability of clay in vertical openings. Journal of the Geotechnical Engineering Division, ASCE 1967; 193:71–94.
[20] Atkinson JH, Mair RJ. Soil mechanics aspects of soft ground tunnelling. Ground Engineering 1981;14:20–4.
[21] Sloan SW. Lower bound limit analysis using finite elements and linear programming. International Journal for Numerical and Analytical Methods in Geomechanics 1988;12:61–77.
[22] Lyamin AV. Three-dimensional lower bound limit analysis using non-linear programming. PhD thesis, Department of Civil, Surveying and Environmental Engineering, University of Newcastle, Australia, 1999.
[23] Lyamin AV, Sloan SW. Lower bound limit analysis using non-linear programming. International Journal for Numerical Methods in Engineering 2002;55:573–611.
[24] Sloan SW. Upper bound limit analysis using finite elements and linear programming. International Journal for Numerical and Analytical Methods in Geomechanics 1989;13:263–82.
[25] Sloan SW, Kleeman PW. Upper bound limit analysis with discontinuous velocity fields. Computer Methods in Applied Mechanics and Engineering 1995;127:293–314.
[26] Lyamin AV, Sloan SW. Upper bound limit analysis using non-linear programming. International Journal for Numerical and Analytical Methods in Geomechanics 2002;26:181–216.
[27] Ewing DJF, Hill R. The plastic constraint of V-notched tension bars. Journal Mech Phys Solids 1967;15:115–24.
[28] Chen WH. Limit analysis and soil plasticity. Amsterdam: Elsevier; 1975.